BMC Genomics

RESEARCH Open Access

Mining candidate genes for meat tenderness in Qinchuan cattle based on transcriptome analysis

Haobin Ma[1], Juntao Guo[1], Jianfang Wang[1], Tongfei He[1], Diba Dedacha Jilo[1], Ziyou Jiao[1], Gong Cheng[1,2*] and Linsen Zan[1,2*]

Abstract

Background Qinchuan cattle, renowned for their distinctive meat quality, flavor, and exceptional environmental adaptability, represent a highly valuable genetic resource in beef cattle breeding. However, the molecular mechanisms underlying the formation of its meat quality traits, especially the genetic regulatory network of the core indicator of tenderness that affects consumer experience, are not yet clear. This study aims to employ transcriptomic techniques to identify candidate genes associated with tenderness in Qinchuan cattle, thereby providing a theoretical foundation for molecular breeding in beef cattle.

Results Phenotypic analysis of meat quality revealed that the average shear force of the longissimus dorsi muscle (LDM) from 20 Qinchuan cattle was 115.43 ± 20.25 N, with significant differences among individuals ($P < 0.01$). Based on extreme tenderness differences, high shear force groups (HSF, $n = 3$) and low shear force groups (LSF, $n = 3$) were selected for transcriptome sequencing. A total of 286 differentially expressed genes (DEGs) were identified. Compared with the low shear force group, 247 genes were up-regulated and 39 genes were down-regulated in the HSF. GO and KEGG enrichment analyses indicated that these genes were significantly enriched in processes such as collagen binding, collagen trimer assembly, PI3K-Akt signaling pathway, and regulation of the actin cytoskeleton. Further protein-protein interaction (PPI) network analysis identified 5 hub genes associated with tenderness: *POSTN*, *BGN*, *COL5A2*, *COL6A1* and *COL6A2*. Functional validation in cells showed that knockdown of *POSTN* expression significantly promoted bovine myoblast differentiation (up-regulation of *MRF4*, *MYOG*, and *MYH3* expression, increase in *MYH3* and *MRF4* proteins), while inhibiting the expression of collagen deposition-related genes (*CCN2* and *LOX*).

Conclusions Through transcriptomic and bioinformatic analyses, this study identified 5 core genes closely associated with meat tenderness in Qinchuan cattle and demonstrated that *POSTN* modulates tenderness formation through its dual role in regulating myogenic differentiation and collagen metabolism. These findings provide critical molecular targets for meat quality improvement in Qinchuan cattle and establish a theoretical foundation for molecular breeding of high-quality beef cattle.

*Correspondence:
Gong Cheng
chenggong@nwafu.edu.cn
Linsen Zan
zanlinsen@163.com

Full list of author information is available at the end of the article

Keywords POSTN, Qinchuan cattle, Tenderness, Transcriptome

Background

The tenderness of meat is a key quality attribute that determines consumer acceptance and satisfaction. As living standards and health awareness rise, beef consumption is shifting from quantity to quality. Beef evaluation encompasses physical attributes such as tenderness, meat color, and water-holding capacity; chemical composition such as protein, intramuscular fat, fatty acids, and amino acids; and processing characteristics such as cooking percentage. Tenderness, characterized by the softness and chewiness of muscle tissue, has become a critical metric for beef assessment [1]. Studies show that shear force is significantly negatively correlated with tenderness within a certain range, serving as an important objective measure [2, 3]. Tenderness is regulated by multiple biological factors, including muscle fiber type, diameter, and density [4, 5]; intramuscular connective tissue, particularly collagen content and cross-linking status; and intramuscular fat deposition. Muscle fiber characteristics, connective tissue properties, and fat content are regarded as the most critical determinants [6, 7]. Current research on the influence of muscle fiber traits and intramuscular fat is relatively comprehensive [8, 9]. Muscle fiber diameter and density, as well as intramuscular fat content, all significantly affect tenderness [10, 11]. Smaller fiber diameter and lower density contribute to higher tenderness [12, 13], while intramuscular fat enhances this trait by infiltrating the perimysial space, improving juiciness and flavor [14]. Improving these characteristics will have significant economic impact on the beef industry.

In recent years, the widespread adoption of high-throughput sequencing has established transcriptomics as one of the core tools for dissecting the molecular mechanisms underlying meat quality [15]. Transcriptome sequencing was performed on the LDM of Wagyu and Chinese grassland red cattle, identifying 388 DEGs—205 up-regulated and 183 down-regulated—and screened candidates such as ACOX1 and ANGPTL4 associated with meat quality [16]. The LDM of Holstein bulls and steers was compared, obtaining 56 DEGs and proposing MYH1, MYH4, MYH10, GADL1, CYP2R1, EEPD1, and SHISA3 as potential markers for the effects of castration on muscle quality [17].

These studies have not only expanded the repository of beef quality-related genes but also highlighted the powerful potential of transcriptomics in uncovering regulatory pathways of important traits. Qinchuan cattle, an outstanding representative of Chinese indigenous cattle breeds, are renowned for their unique flavor and superior meat quality, endowing them with high breeding value and development potential. However, current research on the mechanisms underlying meat quality formation remains relatively limited, particularly regarding the systematic elucidation of key genes and their regulatory networks. This knowledge gap significantly restricts the effective utilization of this breed in high-quality beef cattle breeding programs. Therefore, the present study focused on Qinchuan cattle by measuring shear force and screening extreme shear force groups. Using RNA-Seq technology, we constructed transcriptomic profiles of HSF and LSF, identified differentially expressed genes, and built PPI networks. The study aims to screen candidate genes closely associated with tenderness formation and further validate the biological functions of core genes through cell experiments. These findings will enhance the understanding of the genetic mechanisms underlying meat quality traits in Qinchuan cattle and provide a theoretical basis for molecular design breeding.

Materials and methods

Experimental animals and sample collection

A total of 20 LDM samples from 20 Qinchuan bulls were obtained from the Shaanxi Qinchuan Beef Cattle Breeding Farm. All cattle were raised under uniform fattening standards to approximately 24 months of age. Prior to slaughter, cattle were fasted for 24 h. The cattle were rendered unconscious by electrical stunning, followed by exsanguination, ensuring rapid loss of consciousness and minimizing suffering. Immediately after standardized slaughter, fresh LDM samples were collected from the 12th–13th rib section using cryovials, rapidly snap-frozen in liquid nitrogen, and transferred to a − 80℃ freezer for long-term storage. Following a 24-hour chilling period at 4℃, approximately 1 kg of LDM was collected from the same anatomical location (12th–13th rib section), vacuum-packaged, and stored at − 20℃. After overnight thawing at 4 ℃, meat quality traits were evaluated at the National Beef Cattle Improvement Center, Northwest A&F University. Based on shear force measurements, three samples with the highest and three with the lowest shear force values were selected from the − 80℃ stored samples for RNA-seq analysis.

Shear force measurement

Determined according to NY/T 1180–2006 "Meat Tenderness Measurement - Shear Force Method". A rectangular block of LDM (≥ 6 cm × 3 cm × 3 cm, with muscle- fiber length ≥ 3 cm) was trimmed of visible fascia, sealed in a zip-lock bag (bag mouth upward), and immersed in an 80 °C water-bath. Core temperature was monitored with a MITIR probe thermometer (MITIR, Zhejiang, China); when 70 °C was reached, the sample

was immediately removed. After cooling at 4 °C overnight, cylindrical cores (diameter 1.27 cm) were taken parallel to the muscle-fiber direction using a coring drill, with at least six cores obtained from each sample. Each core was sheared perpendicular to the fiber direction using a TA.XT Plus texture analyzer (Baosheng, Shanghai, China), and the peak shear force was recorded; the average of these values was taken as the shear force of the LDM sample.

Transcriptome sequencing and analysis

Total RNA extraction, library construction, and RNA-seq were performed by Biomarker Technologies (Beijing, China). After RNA quality control, libraries were constructed with the main procedures as follows: eukaryotic mRNA is enriched using magnetic beads with Oligo(dT); Fragmentation Buffer is added to randomly fragment the mRNA; using mRNA as a template, the first strand of cDNA is synthesized with random hexamers, followed by the addition of buffer, dNTPs, RNase H, and DNA polymerase I to synthesize the second strand of cDNA, which is then purified using AMPure XP beads; the purified double-stranded cDNA undergoes end repair, Adenosine, and sequencing adapter ligation, followed by fragment size selection using AMPure XP beads; finally, the cDNA library is obtained through PCR enrichment. Then libraries were quantified using Qubit 2.0, assessed for insert size by Agilent 2100, and validated for effective concentration by qPCR. Qualified libraries were sequenced on a DNBSEQ-T7 platform with paired-end 150 bp reads. Raw sequencing data were filtered using fastp to obtain clean reads, which were aligned to the bovine reference genome ARS_UCD1.3 using Hisat2 v2.2.1 [18]. Gene expression quantification was performed using StringTie v2.1.7 [19] and featureCounts v2.0.6 [20] to obtain FPKM and count values. Differential expression analysis was conducted using DESeq2 v1.42.1 [21], with $|\log2FoldChange| \geq 1$ and $P < 0.01$ as the cutoff for DEGs. GO and KEGG enrichment analyses were performed on DEGs. Finally, DEGs were imported into the STRING database to construct a PPI network, and hub genes and key subnetwork modules were identified using Cytoscape v3.10.2 with the CytoHubba and MCODE plugins. MCODE parameters are set to degree cutoff = 2, max. depth = 100, k-core = 2, and node score cutoff = 0.35; hub genes are screened using the MCC algorithm in the cytoHubba plugin.

Bovine myoblast isolation, culture and induced differentiation

Myoblast isolation was carried out according to the method established in our laboratory [22]. The obtained cells were seeded in growth medium consisting of DMEM-F12 (Gibco, USA), 15% fetal bovine serum (PAN, GER) and 1% penicillin-streptomycin (Gibco, USA) and cultured at 37 °C with 5% CO_2 in a humidified incubator (Thermo Fisher Scientific, USA); the medium was renewed every 48 h. When cell density reached 90–95%, the medium was switched to differentiation medium (DMEM-F12 + 2% horse serum + 1% penicillin-streptomycin) and refreshed every 48 h to induce differentiation.

Small interfering RNA (siRNA) transfection

Small interfering RNA targeting *POSTN* (si-POSTN) was used for gene silencing, with a non-targeting siRNA (si-NC) serving as the negative control. The si-NC sequences were: sense 5'-UUCUCCGAACGUGUCACGUTT-3' and antisense 5'-ACGUGACACGUUCGGAGAATT-3'. The si-POSTN sequences were: sense 5'-CAGAAGAAA CUCUGAAGAATT-3' and antisense 5'-UUCUUCAGA GUUUCUUCUGTT-3'. When myoblast density reached approximately 50%, transfection was performed using 4μL siRNA, 2.5μL Lipofectamine 3000 (Invitrogen, Carlsbad, CA, USA) and 250μL Opti-MEM (Invitrogen, USA). After 24 h, the medium was changed to differentiation medium and refreshed every 48 h, cells were collected on day 4 for subsequent experiments.

RNA extraction and real-time quantitative PCR (RT–qPCR)

LDM tissue samples were ground in liquid nitrogen, and total RNA was extracted using the TRIzol method; the same procedure was applied to isolate RNA from myoblasts. The obtained RNA was reverse-transcribed into cDNA using the Evo M-MLV RT Mix Kit (Agbio, China). Subsequently, amplification was performed with Perfect-Start Green qPCR SuperMix (TransGen Biotech, China) on a CFX Connect real-time fluorescent quantitative PCR system (Bio-Rad, Hercules, CA, USA). *GAPDH* served as the internal reference gene, and relative expression levels were calculated using the $2^{-\Delta\Delta Ct}$ method. Both the control and experimental groups included three biological replicates, and each biological sample was subjected to two technical replicates in RT-qPCR. All RT-qPCR primers were designed using the NCBI Primer-BLAST online tool. The following criteria were applied during design: (i) amplicon length of 100–200 bp; (ii) primer melting temperature (Tm) between 57–63℃, with a Tm difference of no more than 3℃ between forward and reverse primers; and (iii) GC content of 40%–60%. Primer specificity was verified by BLAST alignment against the Bos taurus reference genome to ensure absence of non-specific amplification. All primers were synthesized by Tsingke Biotech Co., Ltd. (Beijing, China), and their sequences are listed in Table S1.

Protein extraction and western blot

After removal of the medium, cells were washed three times with PBS. Each well was then treated with 200μL

of RIPA lysis buffer containing 1% PMSF (Beyotime, Shanghai, China) and incubated on ice for 15 min; cells were scraped and the lysate transferred to a 1.5mL tube. Following centrifugation at 12,000 r·min^{-1} for 10 min at 4 °C, the supernatant was mixed with 5× loading buffer at a ratio of 4:1 and boiled at 100 °C for 10 min for denaturation. Proteins were separated by SDS-PAGE and electro-transferred to a PVDF membrane. After a brief rinse in 1×TBST, the membrane was blocked for 30 min and sequentially incubated with primary antibodies at 4 °C overnight and HRP-conjugated secondary antibodies at room temperature for 2 h in the dark. Chemiluminescence was detected using the DocTMXR system (Bio-Rad, USA). Four primary antibodies were used: GAPDH (1:1,000, BBI, China), MEF2C (1:500, Biorbyt, UK), MRF4 (1:1,000, Proteintech, China), and MYH3 (1:1,000, Proteintech, China); the secondary antibody was HRP-labeled goat anti-rabbit IgG (1:10,000, BBI, China), with GAPDH serving as the loading control. Both the control and experimental groups comprised three biological replicates (independently cultured and treated cell protein samples), and western blotting was performed in triplicate (three technical replicates) to ensure reproducible results.

Immunofluorescence

After washing differentiated myoblasts with PBS, cells were fixed with 4% paraformaldehyde at room temperature for 15 min, rinsed three times with PBS, permeabilised with 0.5% Triton X-100 for 15 min, and blocked with blocking solution (1% BSA, 10% donkey serum, 0.3 M glycine) at room temperature for 1 h. Cells were then incubated with primary antibody anti-Desmin (1:200, Thermo Fisher, China) at 4 °C overnight, washed three times with PBS, and incubated with Alexa Fluor 488-conjugated goat anti-mouse IgG secondary antibody (1:1000, Abcam, UK) at room temperature for 2 h in the dark. Nuclei were stained with Hoechst (1:2000, Beyotime) for 15 min, washed three times with PBS, and images were captured using an inverted fluorescence microscope. The differentiation index was defined as the percentage of nuclei within Desmin-positive myotubes relative to the total number of nuclei, and quantified using ImageJ software. Both the control and experimental groups comprised two biological replicates (independently cultured and treated cell samples), and six random fields were imaged per sample (six technical replicates).

Statistical analysis

Meat-quality data are presented as "mean ± SD" and were analyzed using GraphPad Prism 8 (v8.0.2, GraphPad Software, USA). Comparisons between two groups were performed with Student's two-tailed t-test; differences among group means were evaluated by two-way ANOVA followed by Bonferroni post-hoc tests. The significance level was set at $P < 0.05$ (*) and indicating $P < 0.01$ (**).

Results

Meat quality trait measurements

Shear-force measurements revealed that the mean shear force of LDM from the 20 Qinchuan cattle was 115.43 ± 20.25 N, with a maximum of 143.46 N and a minimum of 89.08 N (Fig. 1A, Table S2), indicating substantial variation within the population. Based on these results, the three individuals with the highest and the three with the lowest shear forces were selected for transcriptome sequencing (Fig. 1B; Table 1): the HSF group recorded 142.71 ± 1.11 N and the LSF group 90.78 ± 1.64 N, the difference being extremely significant ($P < 0.01$).

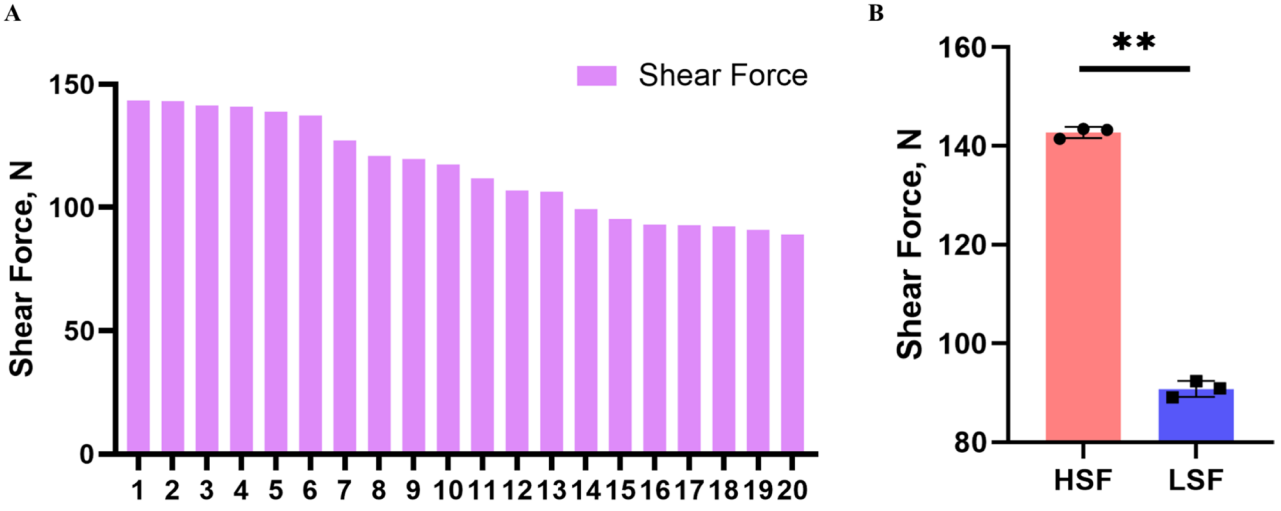

Fig. 1 Shear force measurement. **A** The shear force measurement results of 20 Qinchuan cattle. **B** Comparison of shear forces between HSF and LSF. $^{**}P < 0.01$ indicates extremely significant difference

Table 1 Shear force values of HSF and LSF

group		Shear Force, *N*
High Shear Force	HSF1	143.46
	HSF2	143.24
	HSF3	141.43
Low Shear Force	LSF1	92.35
	LSF2	90.91
	LSF3	89.08
P-value		< 0.0001

Table 2 Quality assessment of sequencing data and sequence alignment

Sample ID	OBtained Base, Gb	Q20, %	Q30, %	GC, %	Mapping Rate, %
HSF1	6.74	98.97	96.65	50.85	99.04
HSF2	6.77	99.08	96.93	50.24	98.37
HSF3	5.72	99.06	96.89	50.46	98.66
LSF1	7.43	98.90	96.48	50.57	98.69
LSF2	6.18	99.19	97.32	51.22	98.63
LSF3	7.18	99.05	96.87	51.08	98.26

Identification of DEGs

A total of 40.02 Gb Clean Data were obtained from the HSF and LSF, with an average of 6.67 Gb per sample and Q30 ≥ 96.48%. All Clean Data were aligned to the ARS_UCD1.3 genome, with alignment rates ≥ 98.26% (Table 2), indicating high data quality. PCA plot showed clear separation between the two groups (Fig. 2A); The expression heatmap showed differential expression patterns of myosin-related genes such as *TPM1*, *TPM2*, *MYL1*, *MYL2*, and *MYL11* between HSF and LSF (Fig. 2B). Using $|\log_2\text{FoldChange}| \geq 1$ and $P < 0.01$ as thresholds, 286 DEGs were identified (Table S3), with 247 genes up-regulated and 39 genes down-regulated for HSF vs. LSF (Fig. 2C). GO enrichment analysis showed these DEGs were related with collagen binding, collagen-containing extracellular matrix, and collagen trimer (Fig. 3A, Table S4); KEGG analysis revealed these DEGs enrichment in PI3K-Akt signaling pathway, regulation of actin cytoskeleton and MAPK signaling pathway (Fig. 3B, Table S5).

PPI network analysis

Given the large number of DEGs, we first constructed a protein–protein interaction network and weighted each node. Hub genes were identified with cytoHubba (Fig. 4A, Table S6), and the three highest-scoring sub-network modules (Ⅰ, Ⅱ, Ⅲ) were extracted using MCODE (Fig. 4B–D, Table S7-S9). Functional enrichment revealed that module Ⅰ is enriched for signal-receptor activity and immune-system processes, together with the FcγR-mediated phagocytosis and Toll-like receptor signaling pathways (Fig. 5A–B, Table S10-S11). Module Ⅱ concentrates on collagen binding, collagen-containing extracellular matrix, collagen trimer, and the PI3K-Akt signaling pathways (Fig. 5C–D, Table S12-S13). Module Ⅲ is enriched for responses to viruses and biotic stimuli, including RIG-I-like and NOD-like receptor signalling (Fig. 5E–F, Table S14-S15). After integrated evaluation, module Ⅱ was designated the target. Intersection of module Ⅱ with the hub-gene list yielded five candidates: *POSTN*, *BGN*, *COL6A1*, *COL6A2* and *COL5A2*. RT-qPCR confirmed the sequencing results and verified data reliability (Fig. 2D); *POSTN* showed the most pronounced expression difference between HSF and LSF, so it was selected for subsequent functional assays.

Knock-down of *POSTN* promotes differentiation of bovine myoblasts

To evaluate the effect of *POSTN* on bovine skeletal muscle development, *POSTN* expression in bovine myoblasts was knocked down using siRNA technology, with an interference efficiency exceeding 80% (Fig. 6A). RT-qPCR results revealed that *POSTN* knock-down extremely significantly up-regulated *MRF4* ($P < 0.01$), *MYOG* ($P < 0.01$) and *MYH3* ($P < 0.01$) (Fig. 6B). Furthermore, western blot analysis demonstrated that MYH3 and MRF4 protein levels were extremely significantly elevated after *POSTN* knock-down ($P < 0.01$) (Fig. 6C, D). Immunofluorescence results showed an extremely significant increase in the number of Desmin-positive cells ($P < 0.01$) and enhanced myotube formation (Fig. 6E, F). Collectively, these findings indicate that suppression of *POSTN* expression promotes bovine myoblast differentiation.

Knock-down of *POSTN* inhibits collagen deposition

To clarify the effect of *POSTN* on collagen synthesis, the expression of collagen-related genes was further examined. The results showed that knock-down of *POSTN* significantly down-regulated the mRNA levels of *CCN2* ($P < 0.05$) and *LOX* ($P < 0.05$) (Fig. 6G), indicating that the collagen synthesis pathway was inhibited and collagen deposition was reduced. Subsequently, the STRING database was used to construct a *POSTN* PPI network (Fig. 6H), which revealed that the POSTN-encoded protein interacted with collagen-related proteins such as TGFB1, BMP1, COL1A1, COL1A2, and COL3A1, further supporting the involvement of *POSTN* in the regulation of collagen deposition.

Discussion

Meat-quality measurements showed that the shear force of LDM from 20 Qinchuan cattle was 115.43 ± 20.25 N, basically consistent with the values reported in the literature for Qinchuan cattle [23], but higher than the shear-force level of Angus beef [24], indicating that there is still considerable room for improvement in tenderness. As a core indicator of beef quality, tenderness is

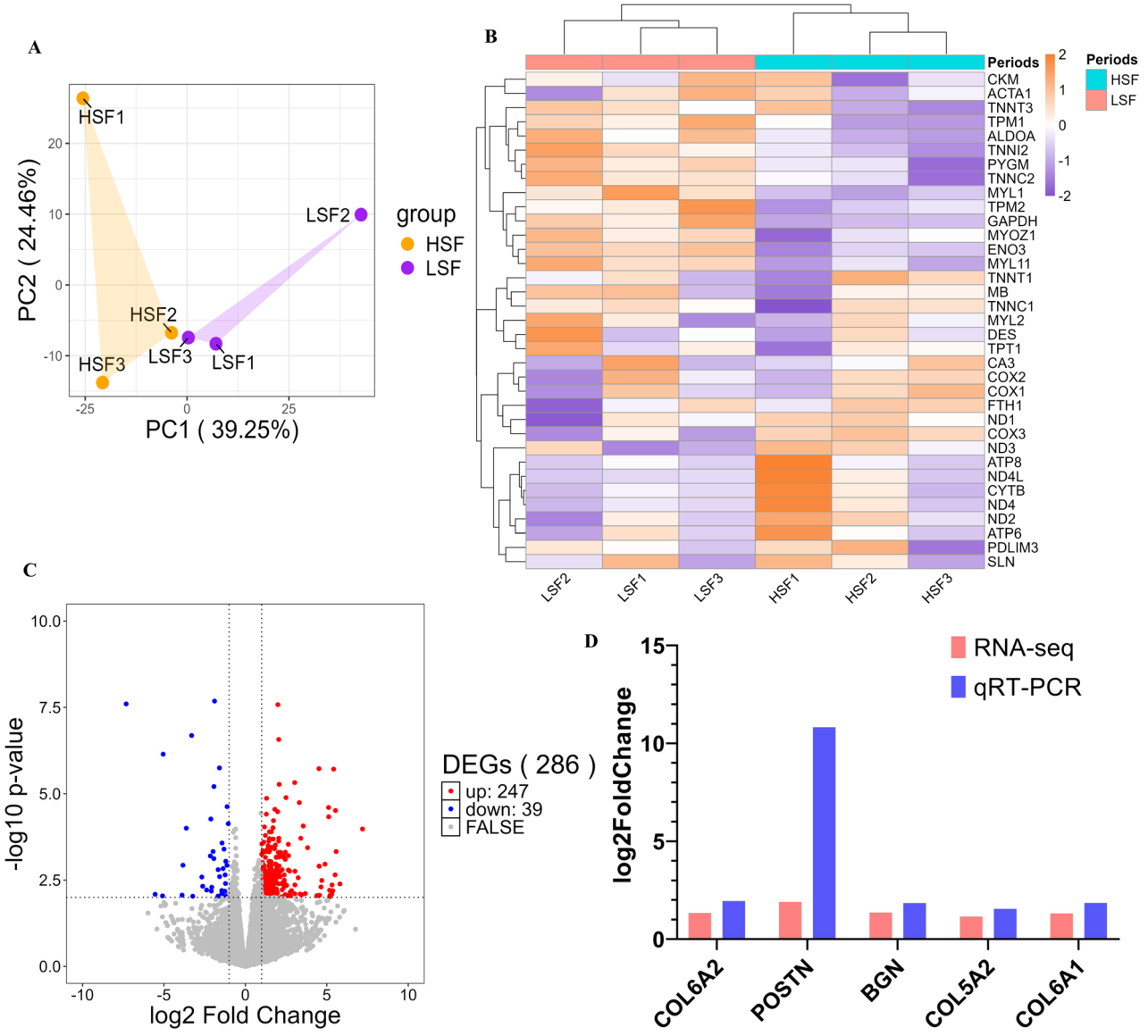

Fig. 2 DEG analysis. **A** PCA of HSF and LSF. **B** Cluster analysis of HSF and LSF. **C** Volcano plot of DEGs. **D**. RT-qPCR validation

significantly affected by factors other than genetic background, such as age, nutritional level, slaughter method, and post-mortem handling (e.g. ageing conditions) [25, 26]. This also suggests that subsequent optimization of feeding duration and post-mortem handling techniques for Qinchuan cattle could further reduce muscle shear force and improve tenderness, thereby enhancing market competitiveness.

To elucidate the molecular regulatory mechanisms underlying the differences between HSF and LSF groups, RNA-Seq was performed on cattle with the most divergent shear force values. A total of 286 DEGs were identified, with 247 up-regulated and 39 down-regulated in the HSF group. Functional enrichment analysis showed that these DEGs were significantly enriched in biological processes such as collagen binding, collagen-containing extracellular matrix, and collagen trimer, indicating their primary involvement in collagen metabolism., indicating that DEGs are mainly related to collagen metabolism. Collagen is the principal component of intramuscular connective tissue, and both its content and degree of cross-linking influence meat tenderness [27]; a higher cross-linking degree leads to lower thermal solubility and tougher meat [28]. Among these, mature inter-molecular cross-links exert a more negative effect on tenderness than collagen content alone [29]. During collagen maturation, intramolecular and intermolecular cross-links are formed sequentially [30] Intramolecular cross-links create bivalent bonds only between two α-chains, yielding an immature structure with low thermal stability [31].

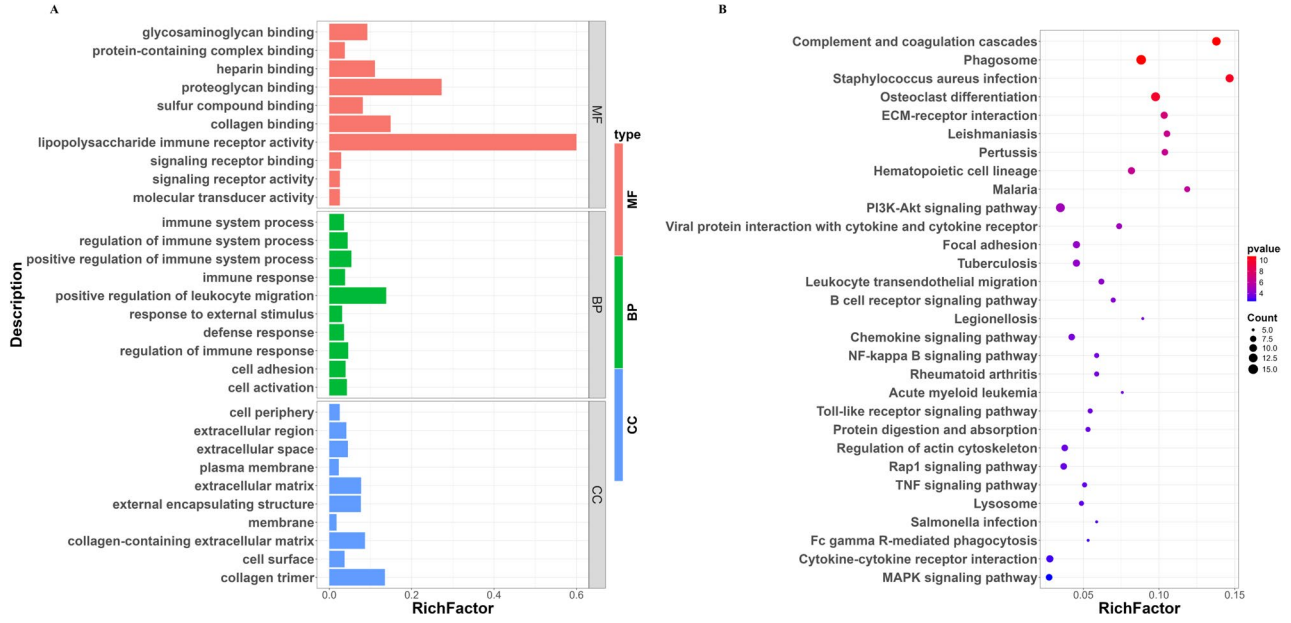

Fig. 3 Functional enrichment analysis of DEGs. **A** GO enrichment analysis of DEGs. **B** KEGG enrichment analysis of DEGs

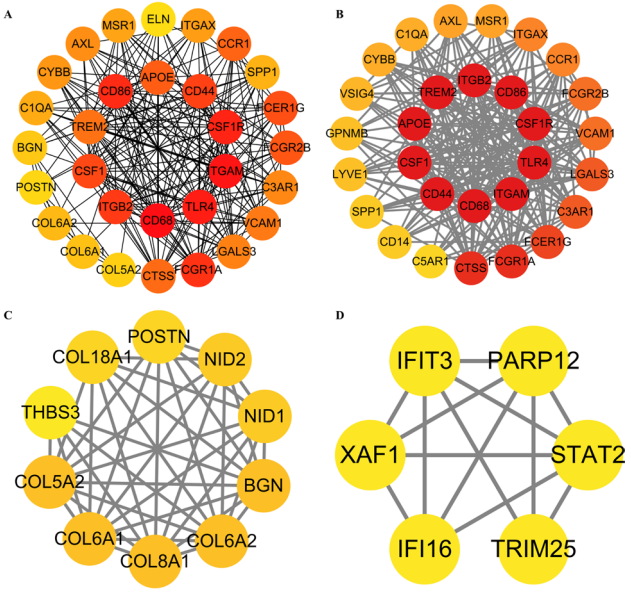

Fig. 4 PPI analysis of DEGs. **A** Proteins encoded by the top 30 hub genes screened by cytoHubba. **B** Proteins encoded by genes in sub-network module Ⅰ. **C** Proteins encoded by genes in sub-network module Ⅱ. **D** Proteins encoded by genes in sub-network module Ⅲ. Each node represents the protein encoded by the corresponding gene; node color is correlated with the Degree value (the number of edges directly connected to the node), with redder colors indicating higher Degree values

When this bivalent linkage further condenses with lysine or hydroxylysine on the α-chain of an adjacent collagen molecule, an intermolecular, trivalent, non-reducible mature cross-link is generated [32]. Mature cross-links between collagen molecules provide connective tissue with requisite physicochemical properties and biological stability. Previous studies have shown that as animal age increases, the number of mature collagen cross-links rises and thermal solubility declines, resulting in greater connective-tissue rigidity and reduced tenderness [6, 31].

The PPI network and key sub-network modules constructed in this study further demonstrated that DEGs were significantly enriched in terms of collagen binding and collagen-containing extracellular matrix. Module II identified five hub genes closely associated with collagen binding: *POSTN*, *BGN*, *COL5A2*, *COL6A1*, and *COL6A2*. Among them, the extracellular matrix (ECM) protein encoded by *POSTN* plays a critical role in collagen fibrillogenesis, cell adhesion, and fibroblast differentiation [33]. Its early expression promotes cell proliferation and collagen synthesis, while cleavage of the C-terminus switches its function to enhancing collagen cross-linking [34]. *POSTN* facilitates collagen cross-linking by binding to bone morphogenetic protein 1 (*BMP1*) and activating the lysyl oxidase (*LOX*) precursor [35]. *BGN* is a leucine-rich small proteoglycan [36] that modifies ECM structure, regulates multiple signaling pathways [37, 38], and directly binds collagen [39]. *COL5A2*, *COL6A1*, and *COL6A2* encode the α2 chain of collagen V and the α1 and α2 chains of collagen VI, respectively, forming the structural basis of the collagen fibrillar network [40]. Collectively, these hub genes provide key targets for elucidating the molecular mechanisms underlying muscle tenderness in Qinchuan cattle by synergistically regulating collagen synthesis, fibril formation, and cross-linking.

In this study, *POSTN* was the most significantly upregulated in HSF, consistent with the report by Leshan Wang that *COL1A1* and *POSTN* expression levels were

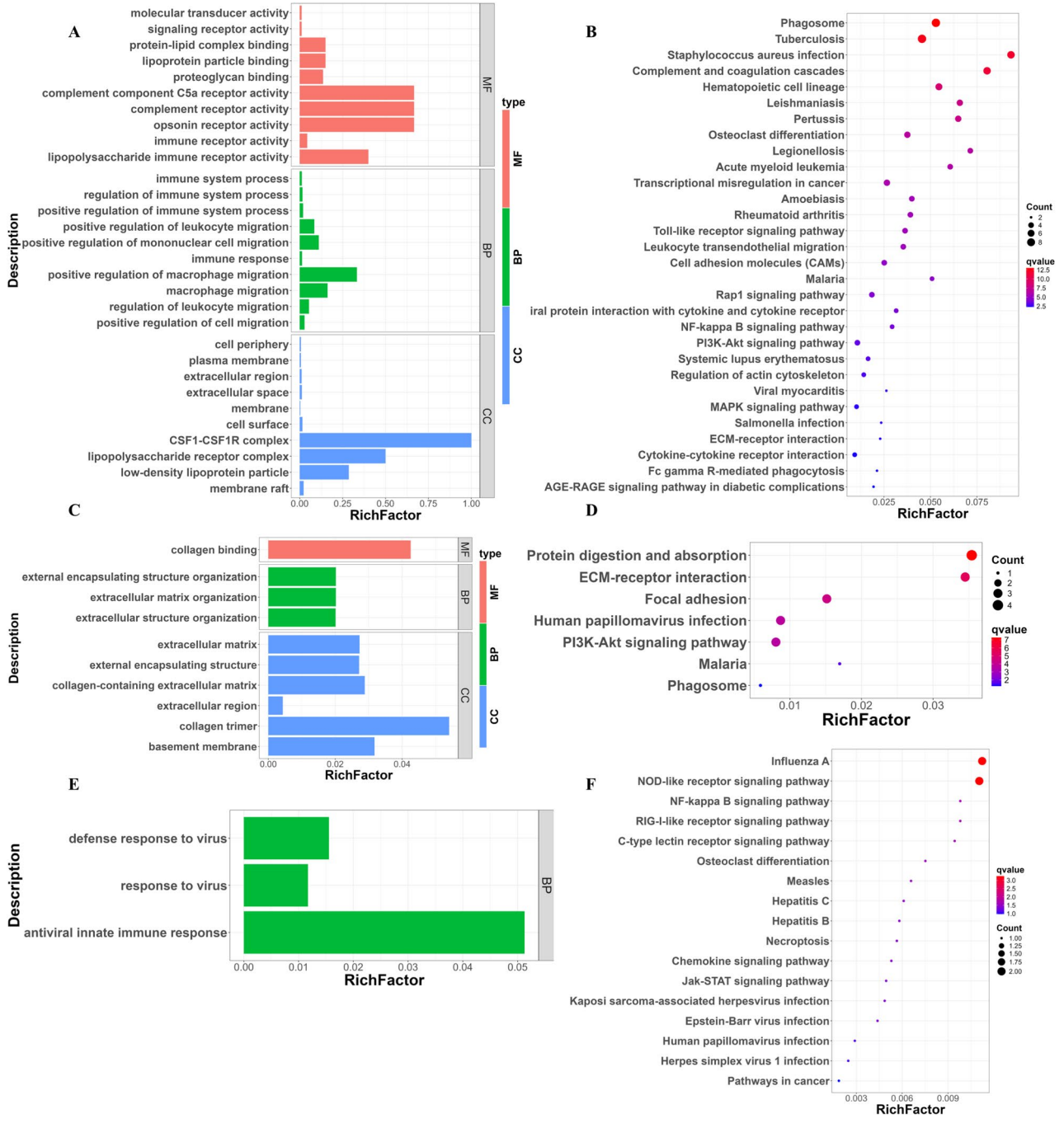

Fig. 5 Functional enrichment analysis of sub-network modules. **A** GO enrichment analysis and (**B**) KEGG enrichment analysis of genes in sub-network module Ⅰ. **C** GO enrichment analysis and (**D**) KEGG enrichment analysis of genes in sub-network module Ⅱ. **E** GO enrichment analysis and (**F**) KEGG enrichment analysis of genes in sub-network module III

higher in the FAP population of Brahman cattle than in Wagyu [41]. Lin Yin also reported that *POSTN* expression was decreased in a mouse model of muscle atrophy [42], matching our trend. However, *POSTN* is markedly elevated in patients and cellular models with myotonic dystrophy type 1 (DM1) [43], a disease characterized by ECM remodeling, fibrosis, and muscle atrophy, which appears contrary to our observation of *POSTN* up-regulation in HSF. Further investigations demonstrated that *POSTN* is induced in fibroblasts within diseased skeletal muscle [44], and *POSTN* is lowly expressed in healthy tissue but up-regulated during acute injury and muscular dystrophy [45], suggesting its involvement in different pathological processes by promoting ECM fibrosis. Additionally, other finding reported found that *POSTN* expression gradually increased during in vitro

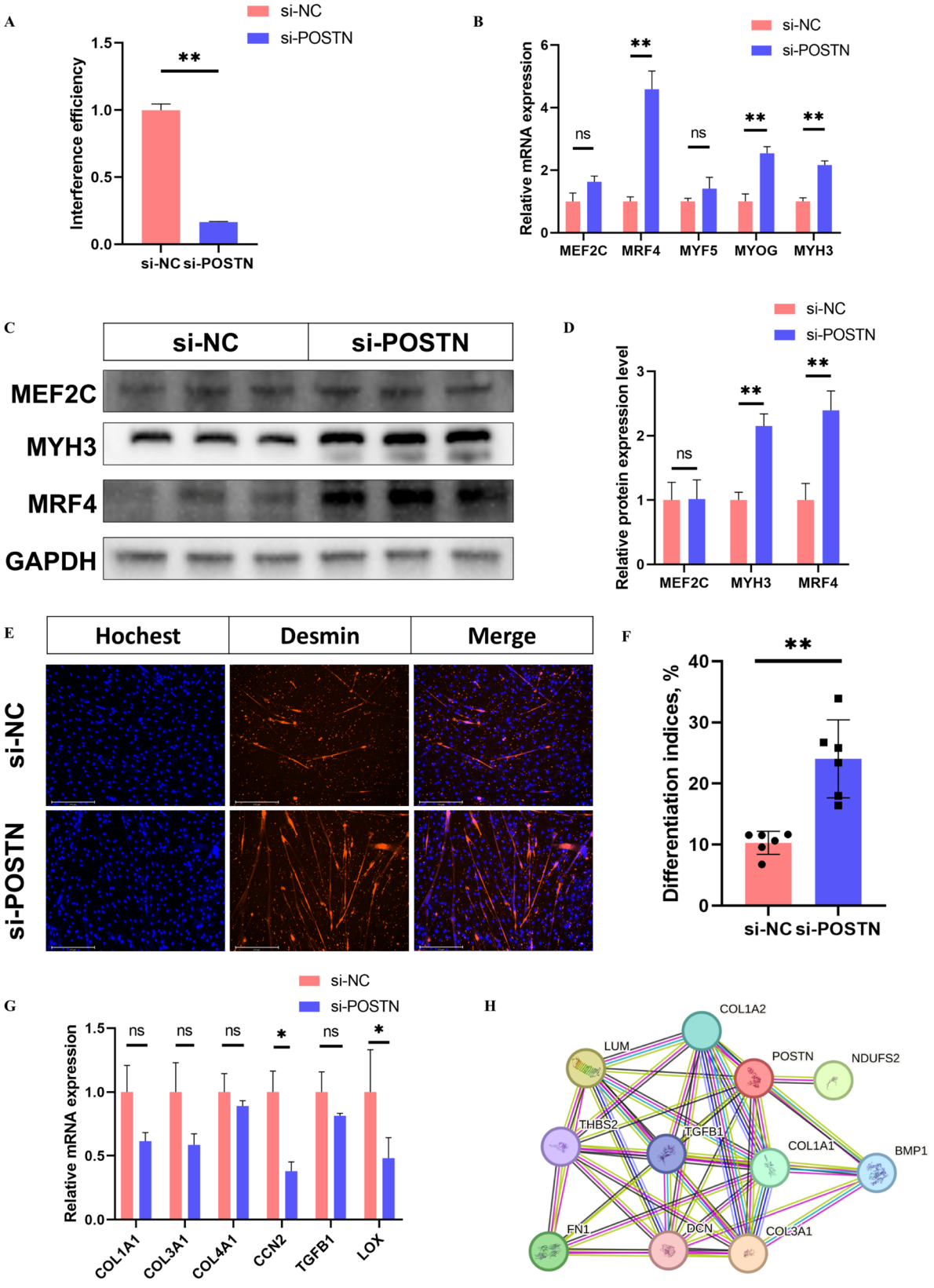

Fig. 6 (See legend on next page.)

(See figure on previous page.)

Fig. 6 Effects of *POSTN* knock-down on cell differentiation and collagen deposition. **A** Interference efficiency of *si-POSTN* in bovine myoblasts. **B** Expression of myogenic differentiation-related mRNAs in bovine myoblasts after *POSTN* knock-down. **C** Western blot analysis of relevant proteins in bovine myoblasts following *POSTN* knock-down. **D** Statistical analysis of protein expression shown in (**C**). **E** Immunofluorescence analysis of *Desmin* expression and localization in si-NC and si-POSTN groups, Bar = 275 μm. **F** Statistical analysis of differentiation index (percentage of nuclei within Desmin-positive myotubes relative to total nuclei) in (**E**), $n = 6$. **G** Expression of collagen-related mRNAs in bovine myoblasts after *POSTN* knock-down. **H** POSTN PPI network constructed using the STRING database

myogenic differentiation, yet inhibition of *POSTN* accelerated myoblast differentiation [43], aligning with our conclusion and indicating that *POSTN*-mediated suppression of myogenic differentiation may coexist with its function in promoting ECM fibrosis. Collectively, we speculate that, compared with its regulation of myoblast differentiation, *POSTN* expression plays a more central role in ECM remodeling and fibrosis.

Therefore, we investigated the effect of knock-down *POSTN* on the differentiation of bovine myoblast cells. We found that knock-down *POSTN* can promote the bovine myoblast differentiation, which is consistent with the findings of Xiaopeng Shen in murine myoblasts [43]. Specifically, the expression levels of *MRF4*, *MYOG* and *MYH3* were extremely significantly elevated, and although *MEF2C* and *MYF5* did not reach statistical significance, their expression levels also exhibited an upward trend. *MRF4* and *MYOG* are myogenic regulatory factor mainly expressed at the late stage of myoblast differentiation, whereas *MYF5* functions primarily during early myoblast differentiation [46, 47]. *MYH3* is a subtype of the myosin heavy chain family and also a typical marker of myogenic differentiation [48]; its up-regulation further confirms that knock-down of *POSTN* promotes myoblast differentiation. Immunofluorescence further demonstrated that the number of Desmin-positive myotubes increased after *POSTN* knock-down. Desmin is the main component of the cytoskeleton of muscle intermediate filaments and is one of the earliest expressed muscle-specific proteins during muscle development [49], its elevated content indicates *POSTN* knock-down enhanced myotube formation. Western blot results showed that *MYH3* and *MRF4* protein levels were extremely significantly up-regulated, a trend consistent with their respective mRNA abundances. Therefore, knock-down *POSTN* can promote bovine myoblast differentiation.

Given that *POSTN* has been shown to participate in collagen cross-linking and deposition, we further examined the expression changes of collagen-related genes after its knock-down. The results showed that the mRNA levels of *CCN2* and *LOX* were significantly down-regulated, while *COL1A1*, *COL3A1*, *COL4A1* and *TGFB1* showed a downward trend but did not reach statistical significance. *LOX* belongs to the copper-dependent amine oxidase family and catalyzes the conversion of lysines and hydroxylysine residues in collagen and elastin into highly reactive aldehydes, which then condense with other oxidized groups or intact lysines to form intra- and inter-molecular cross-links [50, 51]. The mechanism by which *POSTN* promotes the maturation of the *LOX* precursor and accelerates collagen cross-linking via binding to *BMP1* has been elucidated in the previous research and is consistent with the present results. *CCN2* is a secreted matricellular protein that interacts with ECM components such as collagen and promotes ECM deposition through multiple signaling pathways [52]. *TGF-β1* is a key inducer of ECM components (collagen, fibronectin, etc.) [53]; blocking *CCN2* reduces intramuscular *TGF-β1* production [54], and *CCN2* can activate *TGF-β1* signaling by inhibiting BMP signaling [55]. It has also been reported that *TGF-β1* stimulates SMAD3 reporter gene expression and up-regulates *ACTA2*, *COL1A1*, *COL3A1*, *FN1* and *CCN2* [56], while *CCN2* in turn re-activates *TGF-β1* signaling, forming a positive feedback loop [57, 58]. The PPI network revealed that *POSTN* interacts with *TGFB1*, *BMP1*, *COL1A1*, *COL1A2*, *COL3A1*. Numerous studies have confirmed that *POSTN* acts as a downstream effector of *TGF-β1* [59–61]. Therefore, *POSTN* may regulate collagen deposition via the *TGF-β1* signaling axis, a phenomenon that has been verified in mouse models [44] and is similarly observed in bovine myoblasts in this study. In summary, based on in vitro evidence, *POSTN* may be involved in the regulation of collagen cross-linking and deposition: on the one hand, it binds to *BMP1* to promote maturation of the *LOX* precursor and accelerate collagen cross-linking; on the other hand, it may enhance collagen deposition through the *TGF-β1* signaling axis.

A limitation of this study is the small sample size, with only three biological replicates in each of the HSF and LSF, which may constrain the statistical power for detecting differentially expressed genes. To enhance the reliability of the result and mitigate the impact of the limited sample size, we strictly controlled for sample homogeneity: all Qinchuan cattle were maintained under consistent conditions with respect to age, feeding management, and slaughtering procedures, thereby minimizing biological variation unrelated to shear force or tenderness. Furthermore, our data analysis emphasized pathway-level investigation rather than single-gene analysis—specifically, we focused on collagen-related pathways to identify genes potentially associated with tenderness. This pathway-centric strategy helps reduce the instability of gene selection under small-sample conditions [62, 63]. Finally, we conducted rigorous experimental validation of *POSTN*

through a series of in vitro experiments, which provided additional support for the reliability of the transcriptomic data.

In summary, an increasing body of evidence indicates that meat tenderness is influenced by the characteristics of the ECM, particularly collagen content and its degree of cross-linking. The transcriptome analysis of this study identifies collagen-binding-related pathways as the main enriched terms and reveals multiple hub genes closely associated with collagen metabolism, including *POSTN*, *BGN*, *COL5A2*, *COL6A1*, *and COL6A2*. Among them, *POSTN* is a key regulatory factor; functional validation in bovine myoblasts shows that knockdown of *POSTN* promotes myoblast differentiation while reducing collagen cross-linking and deposition, that is, *POSTN* inhibits myogenic differentiation but promotes extracellular matrix fibrosis.

Conclusion

Overall, this study conducted meat phenotype analysis on 20 Qinchuan cattle, screened for extreme tenderness populations, and performed transcriptome analysis to identify 5 core genes closely related to tenderness, including *POSTN*, *BGN*, *COL5A2*, *COL6A1*, *and COL6A2*. These genes are significantly enriched in collagen metabolism related biological processes and the PI3K-Akt signaling pathway. Further functional experiments have shown that *POSTN* may contribute to molecular mechanisms associated with tenderness by simultaneously regulating myogenic differentiation and collagen cross-linking and deposition. This study provides insights into molecular pathways potentially involved in beef tenderness.

Abbreviations

RNA-Seq	RNA sequencing
DEG	Differentially expressed gene
PPI	Protein–protein interaction
LDM	Longissimus dorsi muscle
HSF	High shear-force
LSF	Low shear-force
RT-qPCR	Reverse transcription quantitative PCR
GO	Gene Ontology
KEGG	Kyoto Encyclopedia of Genes and Genomes
Wb	Western blot
ECM	Extracellular matrix
PCA	Principal component analysis

Supplementary Information

The online version contains supplementary material available at https://doi.org/10.1186/s12864-026-12726-7.

Supplementary Material 1.

Supplementary Material 2.

Acknowledgements

Not applicable.

Authors' contributions

Haobin Ma: Conceptualization, Data curation, Formal analysis, Validation, Visualization, Writing – original draft. Juntao Guo: Conceptualization, Data curation, Visualization, Writing – review & editing. Jianfang Wang: Formal analysis, Methodology, Visualization, Writing – review & editing. Tongfei He: Validation. Diba Dedacha Jilo: Writing – original draft. Ziyou Jiao: Validation. Gong Cheng: Conceptualization, Writing – review & editing. Linsen Zan: Funding acquisition, Project administration, Supervision, Writing – review & editing.

Funding

This study was funded by the National Natural Science Foundation of China (2023YFD1300101, 2023YFD1300103), Science and Technology Special Project of the Ministry of Agriculture and Rural Affairs (19240922, 22250059), Shaanxi Livestock and Poultry Breeding Double-chain Fusion Key Project (2022GD-TSLD-46-0102), Key Agricultural Technology Tackling Project of Shaanxi Province (K3031224096).

Data availability

The raw sequence data reported in this paper have been deposited in the Genome Sequence Archive in National Genomics Data Center, China National Center for Bioinformation / Beijing Institute of Genomics, Chinese Academy of Sciences (GSA: CRA030521) that are accessible at https://ngdc.cncb.ac.cn/gsa/browse/CRA030521.

Declarations

Ethics approval and consent to participate

Ethics approval for all animal experiments was granted by the Institutional Animal Care and Use Committee of Northwest A&F University (protocol number: NWAFUCAST2018-167), following the recommendations of the Regulations for the Administration of Affairs Concerning Experimental Animas of China. Animal use and care were in accordance with the ARRIVE guidelines.

Consent for publication

Not applicable.

Competing interests

The authors declare no competing interests.

Author details

[1]College of Animal Science and Technology, Northwest A&F University, Yangling 712100, China
[2]National Beef Cattle Improvement Center, Yangling 712100, China

Received: 10 October 2025 / Accepted: 3 March 2026
Published online: 10 April 2026

References

1. Gao G, Zhang K, Huang P, Zhao X, Li Q, Xie Y, Yin C, Li J, Wang Z, Zhong H, et al. Identification of SNPs Associated with Goose Meat Quality Traits Using a Genome-Wide Association Study Approach. Animals. 2023;13(13):2089.
2. Xu J, Wang Q, Wang Y, Bao M, Sun X, Li Y. Changes in Meat of Hu Sheep during Postmortem Aging Based on ACQUITY UPLC I-Class Plus/VION IMS QTof. Foods. 2024;13(1):174.
3. Zhang D, Yuan C, Guo T, Liu J, Lu Z. Effects of Different Dietary Energy Levels on Development, Quality of Carcass and Meat, and Fatty Acid Profile in Male Lambs. Animals. 2023;13(18):2870.
4. Yang C, Wu L, Guo Y, Li Y, Deng M, Liu D, Liu G, Sun B. Expression profile and bioinformatics analysis of circRNA and its associated ceRNA networks in longissimus dorsi from Lufeng cattle and Leiqiong cattle. BMC Genomics. 2023;24(1):499.
5. Picard B, Gagaoua M. Muscle Fiber Properties in Cattle and Their Relationships with Meat Qualities: An Overview. J Agric Food Chem. 2020;68(22):6021–39.
6. Roy BC, Das C, Aalhus JL, Bruce HL. Relationship between meat quality and intramuscular collagen characteristics of muscles from calf-fed, yearling-fed and mature crossbred beef cattle. Meat Sci. 2021;173:108375.

7. Huang Y, Liu L, Zhao M, Zhang X, Chen J, Zhang Z, Cheng X, Ren C. Feeding regimens affecting carcass and quality attributes of sheep and goat meat - A comprehensive review. Anim bioscience. 2023;36(9):1314–26.
8. Ertbjerg P, Puolanne E. Muscle structure, sarcomere length and influences on meat quality: A review. Meat Sci. 2017;132:139–52.
9. Chun CKY, Wu W, Welter AA, O'Quinn TG, Magnin-Bissel G, Boyle DL, Chao MD. A preliminary investigation of the contribution of different tenderness factors to beef loin, tri-tip and heel tenderness. Meat Sci. 2020;170:108247.
10. Cai C, Xu J, Huang Y, Lan X, Lei C, Yang X, Xie J, Li Y, Chen H. Differential Expression of ACTL8 Gene and Association Study of Its Variations with Growth Traits in Chinese Cattle. Animals. 2019;9(12):1068.
11. Deng L, Li W, Liu W, Liu Y, Xie B, Groenen MAM, Madsen O, Yang X, Tang Z. Integrative metabolomic and transcriptomic analysis reveals difference in glucose and lipid metabolism in the longissimus muscle of Luchuan and Duroc pigs. Front Genet. 2023;14:1128033.
12. Long Y, Zhang N, Bi Y, Ma T, Paengkoum P, Xiao W, Zhao Y, Yuan C, Wang D, Yang Y, et al. Integrated transcriptomic analysis unveils molecular mechanisms regulating meat quality in newly improved black goat breeds. NPJ Sci food. 2025;9(1):129.
13. Mo M, Zhang Z, Wang X, Shen W, Zhang L, Lin S. Molecular mechanisms underlying the impact of muscle fiber types on meat quality in livestock and poultry. Front veterinary Sci. 2023;10:1284551.
14. Wang Y, Diao K, Li H, Zhang C, Zhang G, Guo C. Effects of Dietary Protein Levels on Production Performance, Meat Quality Traits, and Gut Microbiome of Fatting Dezhou Donkeys. Microorganisms. 2025;13(6):1388.
15. Muniz MMM, Fonseca LFS, Dos Santos Silva DB, de Oliveira HR, Baldi F, Chardulo AL, Ferro JA, Cánovas A, de Albuquerque LG. Identification of novel mRNA isoforms associated with meat tenderness using RNA sequencing data in beef cattle. Meat Sci. 2021;173:108378.
16. Li G, Yang R, Lu X, Liu Y, He W, Li Y, Yu H, Qin L, Cao Y, Zhao Z, et al. RNA-Seq Analysis Identifies Differentially Expressed Genes in the Longissimus dorsi of Wagyu and Chinese Red Steppe Cattle. Int J Mol Sci. 2022;24(1):387.
17. Li Y, Wang M, Li Q, Gao Y, Li Q, Li J, Cao Y. Transcriptome profiling of longissimus lumborum in Holstein bulls and steers with different beef qualities. PLoS ONE. 2020;15(6):e0235218.
18. Kim D, Langmead B, Salzberg SL. HISAT: a fast spliced aligner with low memory requirements. Nat Methods. 2015;12(4):357–60.
19. Pertea M, Pertea GM, Antonescu CM, Chang TC, Mendell JT, Salzberg SL. StringTie enables improved reconstruction of a transcriptome from RNA-seq reads. Nat Biotechnol. 2015;33(3):290–5.
20. Liao Y, Smyth GK, Shi W. featureCounts: an efficient general purpose program for assigning sequence reads to genomic features. Bioinformatics. 2014;30(7):923–30.
21. Love MI, Huber W, Anders S. Moderated estimation of fold change and dispersion for RNA-seq data with DESeq2. Genome Biol. 2014;15(12):550.
22. Wang YN, Yang WC, Li PW, Wang HB, Zhang YY, Zan LS. Myocyte enhancer factor 2A promotes proliferation and its inhibition attenuates myogenic differentiation via myozenin 2 in bovine skeletal muscle myoblast. PLoS ONE. 2018;13(4):e0196255.
23. Yu H, Yang Z, Wang J, Li H, Li X, Liang E, Mei C, Zan L. Identification of key genes and metabolites involved in meat quality performance in Qinchuan cattle by WGCNA. J Integr Agric. 2024;23(11):3923–37.
24. Mateescu RG, Garrick DJ, Garmyn AJ, VanOverbeke DL, Mafi GG, Reecy JM. Genetic parameters for sensory traits in longissimus muscle and their associations with tenderness, marbling score, and intramuscular fat in Angus cattle1. J Anim Sci. 2015;93(1):21–7.
25. Qu H, Ning J, Gao J, Jiao X, Liu X. Effects of Nitric Oxide-Enhanced Pediococcus pentosaceus YT2 on Post-Mortem Beef Tenderization. J Agric Food Chem. 2025;73(22):13843–51.
26. Yar MK, Jaspal MH, Ali S, Badar IH, Ijaz M, Hussain J. Muscle-Specific Effects of Genotype, Animal Age, and Wet Aging Duration on Beef Color, Tenderness, and Sensory Characteristics. Animals. 2024;14(24):3593.
27. Han H, Kuai Z, Yao Z, Lei X, Shi H, Li J, Liu K, Yin H, Wang Y, Quan K. Exploring the influence of sex and age on the quality and flavor of Huai goat longissimus thoracis et lumborum through transcriptomic and metabolomic analyses. BMC Genomics. 2025;26(1):684.
28. Chang X, Xu Y, Cheng L, Yi K, Gu X, Luo Z, Zhang J, Wang J, Geng F. Quantitative proteomic analysis of cattle-yak and yak longissimus thoracis provides insights into the differential mechanisms of meat quality. Food Res Int. 2023;173:113253.
29. da Silva JC, Silva LHP, de Souza MV, Coelho PGB, de Castro Nunes CL, da Silva W, Assis DEF, da Silva Martins T, Chizzotti ML, Guimarães SEF. Characteristics of intramuscular collagen in calf-fed Nellore bulls and steers throughout the finishing phase. Meat Sci. 2023;206:109347.
30. Al-u'datt Da, Allen BG, Nattel S. Role of the lysyl oxidase enzyme family in cardiac function and disease. Cardiovascular Res. 2019;115(13):1820–37.
31. Roy BC, Bruce HL. Contribution of intramuscular connective tissue and its structural components on meat tenderness-revisited: a review. Crit Rev Food Sci Nutr. 2024;64(25):9280–310.
32. Bruce HL, Roy BC, Meat science and muscle biology symposium: biological influencers of meat palatability. : Production factors affecting the contribution of collagen to beef toughness1,2. J Anim Sci. 2019;97(5):2270–2278.
33. Han JM, Kim MH, Choi Y, Kim G, Yang WM. Exploring the Potential Effects and Mechanisms of Asarum sieboldii Radix Essential Oil for Treatment of Asthma. Pharmaceutics. 2022;14(3):558.
34. Kudo A. Introductory review: periostin—gene and protein structure. Cell Mol Life Sci. 2017;74(23):4259–68.
35. Maruhashi T, Kii I, Saito M, Kudo A. Interaction between periostin and BMP-1 promotes proteolytic activation of lysyl oxidase. J Biol Chem. 2010;285(17):13294–303.
36. Dunkman AA, Buckley MR, Mienaltowski MJ, Adams SM, Thomas SJ, Satchell L, Kumar A, Pathmanathan L, Beason DP, Iozzo RV, et al. The tendon injury response is influenced by decorin and biglycan. Ann Biomed Eng. 2014;42(3):619–30.
37. Nastase MV, Young MF, Schaefer L. Biglycan: a multivalent proteoglycan providing structure and signals. J Histochem Cytochem. 2012;60(12):963–75.
38. Darrieutort-Laffite C, Beach ZM, Weiss SN, Eekhoff JD, Soslowsky LJ. Knockdown of biglycan reveals an important role in maintenance of structural and mechanical properties during tendon aging. J Orthop Res. 2023;41(10):2287–94.
39. Schönherr E, Witsch-Prehm P, Harrach B, Robenek H, Rauterberg J, Kresse H. Interaction of Biglycan with Type I Collagen (*). J Biol Chem. 1995;270(6):2776–83.
40. Benati D, Cattin E, Corradi F, Ferrari T, Pedrazzoli E, Patrizi C, Marchionni M, Bertorelli R, De Sanctis V, Merlini L, et al. Restored Collagen VI Microfilaments Network in the Extracellular Matrix of CRISPR-Edited Ullrich Congenital Muscular Dystrophy Fibroblasts. Biomolecules. 2024;14(11):1412.
41. Wang L, Gao P, Li C, Liu Q, Yao Z, Li Y, Zhang X, Sun J, Simintiras C, Welborn M, et al. A single-cell atlas of bovine skeletal muscle reveals mechanisms regulating intramuscular adipogenesis and fibrogenesis. J cachexia sarcopenia muscle. 2023;14(5):2152–67.
42. Yin L, Wu S, Bai P, Wang X. Combination of transcriptomics and proteomics for analyzing potential biomarker and molecular mechanism underlying skeletal muscle atrophy. J Proteom. 2024;309:105283.
43. Shen X, Liu Z, Wang C, Xu F, Zhang J, Li M, Lei Y, Wang A, Bi C, Zhu G. Inhibition of Postn Rescues Myogenesis Defects in Myotonic Dystrophy Type 1 Myoblast Model. Front cell Dev biology. 2021;9:710112.
44. Lorts A, Schwanekamp JA, Baudino TA, McNally EM, Molkentin JD. Deletion of periostin reduces muscular dystrophy and fibrosis in mice by modulating the transforming growth factor-β pathway. Proc Natl Acad Sci USA. 2012;109(27):10978–83.
45. Long AM, Kwon JM, Lee G, Reiser NL, Vaught LA, O'Brien JG, Page PGT, Hadhazy M, Reynolds JC, Crosbie RH, et al. The extracellular matrix differentially directs myoblast motility and differentiation in distinct forms of muscular dystrophy: Dystrophic matrices alter myoblast motility. Matrix Biol. 2024;129:44–58.
46. Hernández-Hernández JM, García-González EG, Brun CE, Rudnicki MA. The myogenic regulatory factors, determinants of muscle development, cell identity and regeneration. Semin Cell Dev Biol. 2017;72:10–8.
47. Asfour HA, Allouh MZ, Said RS. Myogenic regulatory factors: The orchestrators of myogenesis after 30 years of discovery. Experimental biology Med (Maywood NJ). 2018;243(2):118–28.
48. Ye J, Zhao X, Xue H, Zou X, Liu G, Deng M, Sun B, Guo Y, Liu D, Li Y. RNA-Seq Reveals miRNA and mRNA Co-regulate Muscle Differentiation in Fetal Leizhou Goats. Front veterinary Sci. 2022;9:829769.
49. Moneo-Corcuera D, Viedma-Poyatos Á, Stamatakis K, Pérez-Sala D. Desmin Reorganization by Stimuli Inducing Oxidative Stress and Electrophiles: Role of Its Single Cysteine Residue. Antioxid (Basel Switzerland). 2023;12(9):1703.
50. Yi X, Zhou Y, Chen Y, Feng X, Liu C, Jiang DS, Geng J, Li X, Jiang X, Fang ZM. The Expression Patterns and Roles of Lysyl Oxidases in Aortic Dissection. Front Cardiovasc Med. 2021;8:692856.
51. Grau-Bové X, Ruiz-Trillo I, Rodriguez-Pascual F. Origin and evolution of lysyl oxidases. Sci Rep. 2015;5:10568.

52. Brigstock DR. Connective tissue growth factor (CCN2, CTGF) and organ fibrosis: lessons from transgenic animals. J cell communication Signal. 2010;4(1):1–4.
53. Alnahhas N, Pouliot E, Saucier L. The hypoxia-inducible factor 1 pathway plays a critical role in the development of breast muscle myopathies in broiler chickens: a comprehensive review. Front Physiol. 2023;14:1260987.
54. Barbe MF, Hilliard BA, Amin M, Harris MY, Hobson LJ, Cruz GE, Popoff SN. Blocking CTGF/CCN2 reduces established skeletal muscle fibrosis in a rat model of overuse injury. FASEB J. 2020;34(5):6554–69.
55. Abreu JG, Ketpura NI, Reversade B, De Robertis EM. Connective-tissue growth factor (CTGF) modulates cell signalling by BMP and TGF-beta. Nat Cell Biol. 2002;4(8):599–604.
56. Randall LJ, Bajan S, Tran TD, Harvey RJ, Russell FD. Propolis compound inhibits profibrotic TGF-β1/SMAD signalling in human fibroblasts. Sci Rep. 2025;15(1):27260.
57. Lipson KE, Wong C, Teng Y, Spong S. CTGF is a central mediator of tissue remodeling and fibrosis and its inhibition can reverse the process of fibrosis. Fibrogenesis tissue repair. 2012;5(Suppl 1):S24.
58. Shimizu M, Yoshimatsu G, Morita Y, Tanaka T, Sakata N, Tagashira H, Wada H, Kodama S. Rescue of murine hind limb ischemia via angiogenesis and lymphangiogenesis promoted by cellular communication network factor 2. Sci Rep. 2023;13(1):20029.
59. Yu M, Luo D, Qiao J, Guo J, He D, Jin S, Tang L, Wang Y, Shi X, Mao J, et al. A hierarchical bilayer architecture for complex tissue regeneration. Bioactive Mater. 2022;10:93–106.
60. Walker JT, McLeod K, Kim S, Conway SJ, Hamilton DW. Periostin as a multifunctional modulator of the wound healing response. Cell Tissue Res. 2016;365(3):453–65.
61. Roh SY, Kim JY, Cha HK, Lim HY, Park Y, Lee KN, Shim J, Choi JI, Kim YH, Son GH. Molecular Signatures of Sinus Node Dysfunction Induce Structural Remodeling in the Right Atrial Tissue. Mol Cells. 2020;43(4):408–18.
62. Zhou X, Liu J. A computational model to predict bone metastasis in breast cancer by integrating the dysregulated pathways. BMC Cancer. 2014;14:618.
63. Yang Y, Chen Y, Hu L, Zhang C, Chen G, Hou L, Xu Q, Wang Y, Li M. Molecular regulation of whole genome DNA methylation in heat stress response of dairy cows. BMC Genomics. 2025;26(1):464.

Publisher's Note